Subcellular localization of Nox4 and regulation in diabetes

Karen Block[a,1], Yves Gorin[a,1], and Hanna E. Abboud[a,b,2]

[a]Department of Medicine, University of Texas Health Science Center, San Antonio, TX 78229; and [b]Audie Leon Murphy Memorial Hospital Division, South Texas Veterans Health Care System, San Antonio, TX 78229

Edited by Irwin Fridovich, Duke University, Durham, NC, and approved July 14, 2009 (received for review June 22, 2009)

Oxidative stress is implicated in human diseases. Some of the oxidative pathways are harbored in the mitochondria. NAD(P)H oxidases have been identified not only in phagocytic but also in somatic cells. Nox4 is the most ubiquitous of these oxidases and is a major source of reactive oxygen species (ROS) in many cell types and in kidney tissue of diabetic animals. We generated specific Nox4 antibodies, and found that Nox4 localizes to mitochondria. (*i*) Immunoblot analysis in cultured mesangial cells and kidney cortex revealed that Nox4 is present in crude mitochondria, in mitochondria-enriched heavy fractions, and in purified mitochondria; (*ii*) immunofluorescence confocal microscopy also revealed that Nox4 localizes with the mitochondrial marker Mitotracker; and (*iii*) the mitochondrial localization prediction program MitoProt indicated that the probability score for Nox4 is identical to mitochondrial protein cytochrome *c* oxidase subunit IV. We also show that in purified mitochondria, siRNA-mediated knockdown of Nox4 significantly reduces NADPH oxidase activity in pure mitochondria and blocks glucose-induced mitochondrial superoxide generation. In a rat model of diabetes, mitochondrial Nox4 expression is increased in kidney cortex. Our data provide evidence that a functional Nox4 is present and regulated in mitochondria, indicating the existence of a previously undescribed source of ROS in this organelle.

kidney | mitochondria | oxidative stress

Oxidative stress has been implicated in diverse human diseases, including diabetes, atherosclerosis, neurodegenerative diseases, and aging (1–4). The bulk of oxidative pathways are harbored in the mitochondria, where various redox carriers leak electrons to oxygen to form superoxide anion (2–6). However, in phagocytic cells membrane-bound gp91^{phox}-based NAD(P)H oxidase has long been recognized as a major source of reactive oxygen species (ROS) (7). More recently, several isoforms of gp91^{phox}, called Nox proteins, have been cloned and identified in somatic cells (7–9). Nox4 was cloned from the kidney (10), and we and others have recently shown that it is a major source of ROS in renal cells and tissue of diabetic animals (11). Using well-characterized Nox4 antibodies generated in our laboratory (Fig. S1), we found that Nox4 localizes to membranes and mitochondria and is regulated in the kidney cortex in diabetes.

Results and Discussion

Several approaches were used to confirm Nox4 localization. First, crude subcellular fractions were prepared from rat kidney cortex homogenates (12). Immunoblot analysis using the rabbit polyclonal anti-Nox4 antibodies shows that a 70- to 75-kDa band corresponding to Nox4 localizes in both crude membrane (Mb) and mitochondrial fractions (Mit) (Fig. 1*A Upper*). Note that in some mitochondrial preparations, we observed multiple Nox4-immunoreactive bands (Fig. 1*A Lower*). Similar results were obtained by using a commercial Nox4 antibody raised to an epitope of the amino terminus of Nox4 (Fig. S2*A*). The two Nox4 antibodies were generated against different epitopes. Importantly, in the Mit fraction, both antibodies recognize predominant bands at 70–75 kDa. Detection of multiple bands in the Mit fraction is likely due to processing of proteins imported to the mitochondria such as

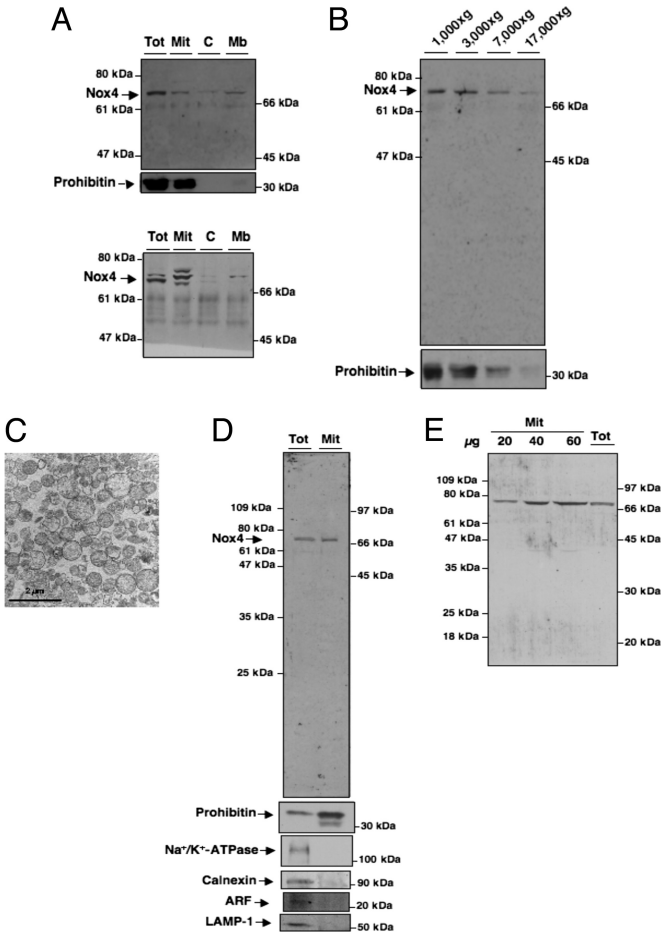

Fig. 1. Subcellular localization of Nox4 in rat kidney cortex. (*A*) Nox4 protein or prohibitin was detected by Western blot analysis in crude subcellular fractions isolated from rat kidney cortex, Total (Tot), Mit, C, or Mb. (*B*) Immunoblotting of subcellular Mb fractions of rat kidney cortex with Nox4 antibody. Prohibitin was used as a marker for mitochondria. (*C*) Electron microscopy of freshly isolated pure mitochondria from kidney cortex. (Scale bar, 2 μm.) (*D*) Immunoblotting of pure Mit (Mit) and total cortical homogenate (Tot) with Nox4 antibody, prohibitin, Na^+/K^+-ATPase, calnexin, ARF, or LAMP-1. (*E*) Western blot analysis of homogenates from Tot and Percoll-purified Mit fractions increasing protein concentrations by using our Nox4 antibody.

Author contributions: K.B., Y.G., and H.E.A. designed research; K.B., Y.G., and H.E.A. performed research; K.B. and Y.G. contributed new reagents/analytic tools; K.B., Y.G., and H.E.A. analyzed data; and K.B., Y.G., and H.E.A. wrote the paper.

The authors declare no conflict of interest.

This article is a PNAS Direct Submission.

[1]K.B. and Y.G. contributed equally to this work.

[2]To whom correspondence should be addressed. E-mail: abboud@uthscsa.edu.

This article contains supporting information online at www.pnas.org/cgi/content/full/0906805106/DCSupplemental.

CELL BIOLOGY

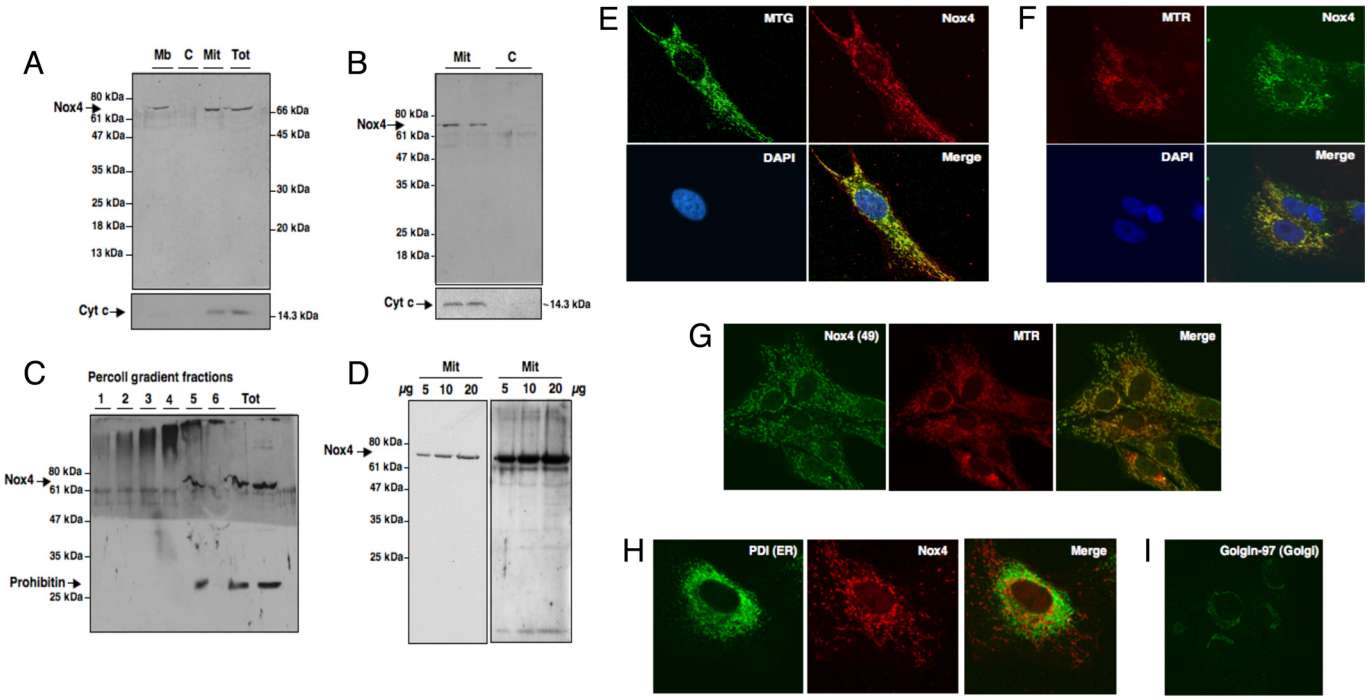

Fig. 2. Subcellular localization of Nox4 in cultured rat MCs. (*A*) Nox4 protein or Cyt *c* was detected by Western blot analysis in 1/5th vol of crude subcellular fractions, Tot, Mit, C, or Mb. (*B*) Mit were isolated by using a mitochondria purification kit (Pierce). Nox4 protein or Cyt *c* was detected by Western blot analysis. C, Cytosolic fraction. (*C*) Pure mitochondria were isolated by using differential centrifugation and Percoll gradient. Fractions were collected, and immunoblotting of each fraction was performed with Nox4 or prohibitin antibodies. Also shown is the immunoblotting of the total cell homogenate. (*D*) Increasing protein concentration of pure Mit fraction were immunoblotted with Nox4 antibody. (*E*) MC mitochondria were labeled with MTG, fixed, permeabilized, and stained by using our Nox4 antibody and a Cyanin-3-linked donkey anti-rabbit secondary antibody. Nuclei were counterstained by using the dye DAPI. (*F*) MC mitochondria were visualized with MTR and then stained with our Nox4 antibody by using a FITC-linked donkey anti-rabbit secondary antibody. Nuclei were counterstained with DAPI. (*G*) MC mitochondria were labeled with MTR and stained with a commercial rabbit anti-Nox4 antibody and Cyanin-3-linked secondary antibody. The color of the overlay was assigned as red and green respectively. (*H*) Endoplasmic reticulum (ER) was stained by using an antibody directed against the marker PDI labeled with Alexa Fluor 488 dye. (*I*) Golgi apparatus was stained by using Golgin-97 as marker and appropriate secondary antibody.

clipping, oxidation or sumoylation that can affect their electrophoretic mobility (13–16). The detection of multiple bands by Nox4 antibody in the total fractions is consistent with the existence of isoforms of Nox4 previously reported by Goyal et al. (17). However, further characterization of these variants is needed. The rabbit antibody generated in the laboratory predominantly recognizes the 70- to 75-kDa band that is also detected by the commercial antibody. In Fig. 1*B*, the Nox4 antibody was used to analyze Nox4 protein expression in fractions of rat renal cortex membranes prepared at different gravitational forces as reported (18). Nox4 is predominantly present in the 1,000, 3,000, and 7,000 $\times g$, heavy Mit fractions. Immunoblotting using prohibitin antibodies, a mitochondrial marker, confirmed that these fractions are enriched in mitochondria (Fig. 1*B*). Nox4, as expected, was also detected to a lesser extent in the 17,000 $\times$ *g* pellet, a fraction enriched in plasma membranes (Fig. 1*B*). Prohibitin was not detected in the pellet, excluding mitochondrial contamination of this fraction. Pure mitochondria were also prepared from rat kidney cortex by using a combination of differential and Percoll gradient centrifugation (19). The brown mitochondrial band was directly collected, and the purity of the preparation was confirmed by electron microscopy, where mostly intact mitochondria are seen (Fig. 1*C*). To further demonstrate that Nox4 is localized within the mitochondria, Percoll gradient-purified mitochondria were resolved by SDS/PAGE and probed for Nox4. Western blot analyses showed that mitochondrial Nox4 expression is robust (Fig. 1*D*). The purity of mitochondria from kidney cortex was determined by the expression of prohibitin (mitochondria) and the absence of Na^+/K^+-ATPase (plasma membrane), calnexin (endoplasmic reticulum), ADP ribosylation factor (ARF; Golgi), or LAMP-1 (lysosome) (Fig. 1*D*). Titration of the pure Mit fraction confirms that our Nox4 antibody predominantly detects the 70- to 75-kDa band (Fig. 1*E*). Mitochondrial Nox4 expression was verified in the total and Percoll gradient-purified mitochondria fractions by using a commercial antibody (Fig. S2*B*).

We also investigated the mitochondrial localization of Nox4 in rat kidney glomerular mesangial cells (MCs), vascular pericytes known to express an active Nox4-based superoxide generating NAD(P)H oxidase (11). MCs constitute a primary target for glucose-mediated oxidative injury (11). Differential centrifugation of MC extracts yielded several subcellular fractions that were probed for Nox4. Similar to kidney cortex, Nox4 was detected as a 70- to 75-kDa protein in crude Mit and Mb fractions (Fig. 2*A*). The mitochondrial extract was positive for the mitochondrial-specific protein cytochrome (Cyt) c, by immunoblotting (Fig. 2*A*). Mitochondria were also isolated by using a Mit fractionation kit that allowed the fractionation of MCs into cytosol (C) and mitochondria (Mit) (Fig. 2*B*). Western blot analysis showed that in MCs, Nox4 localizes to mitochondria, but not to C (Fig. 2*B*), similar to the above findings in kidney cortex. As described in the studies with kidney cortex, purified mitochondria were also obtained by Percoll gradient centrifugation of the crude mitochondria fraction. In this set of experiments, the mitochondrial band was collected by gradient fractionation. Nox4 was exclusively detected in fraction 5, which also expresses the mitochondrial marker prohibitin (Fig. 2*C*; Fig. S3). Immunoblot analysis with increasing amounts of pure mitochondria isolated from MCs also yielded a predominant 70- to 75-kDa band (Fig. 2*D*). These results demonstrate that Nox4 cofractionates with purified mitochondria in MCs.

Immunofluorescence confocal microscopy was also used to localize Nox4 in MCs by using Cyanin-3-labeled or FITC-

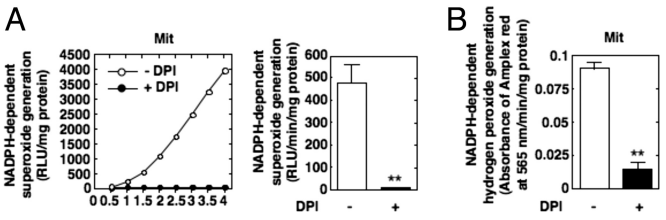

Fig. 3. Nox activity in mitochondria. NADPH oxidase activity was assessed in Percoll gradient-purified mitochondria isolated from control MCs or cells treated with DPI (5 μM) either by measuring NADPH-dependent superoxide generation with the lucigenin-enhanced chemiluminescence method (*A*) or NADPH-dependent hydrogen peroxide production with Amplex Red reagent (*B*). **, $P < 0.01$ versus control cells. Values are the mean ± SE of three independent experiments.

conjugated anti-rabbit IgG. Nox4 colocalizes with the mitochondrial markers Mitotracker Green FM (MTG) or Mitotracker Deep Red 633 (MTR) (Fig. 2 *E* and *F*, respectively). Some Nox4 also localizes to the plasma cell membrane. Nox4 localization to the mitochondria was independently observed by using commercially available Nox4 antibodies (Fig. 2*G*). In contrast, Nox4 staining had little or no overlap with a marker of endoplasmic reticulum, the protein disulfide isomerase (PDI) (Fig. 2*H*). The comparison of Nox4 staining (Fig. 2 *E*-*G*) with the staining of the Golgi complex marker Golgin-97 (Fig. 2*I*) indicates that Nox4 was not present in this organelle. Immunofluorescence analysis also showed that Nox4 staining overlaps with MTR in other renal cells, including glomerular endothelial (Fig. S4*A*) and epithelial cells (Fig. S4*B*), as well as in nonrenal cells such as aortic endothelial cells (Fig. S4*C*) and vascular smooth muscle cells (Fig. S4*D*), indicating that Nox4 mitochondrial localization was not specific to kidney cells. In summary, confocal immunofluorescence microscopy confirmed colocalization of Nox4 to mitochondria in cultured cells. It should be mentioned that Nox4 was found to localize to various subcellular compartments such as endoplasmic reticulum, focal adhesions, nucleus, and the plasma membrane (20–24). These observations may be due to differences in cell types expressing different Nox4 isoforms and/or different cellular functions that requires the association of Nox4 isoforms with signaling molecules in specific cellular domains (20, 21). However, in the present study, we consistently find that Nox4 localizes to the mitochondria in various cell types. The mitochondrial localization prediction program, MitoProt, was used to evaluate the probabilities of Nox4 mitochondrial localization. The amino acid sequences for the Nox catalytic subunits, Nox4, gp91^{phox}/Nox2, Nox1, and Nox3 were retrieved from the Swiss Prot database and analyzed in the web-based service MitoProt II 1.0a4. There is a strong prediction for mitochondrial localization of Nox4, but not the other Nox isoforms (Table S1).

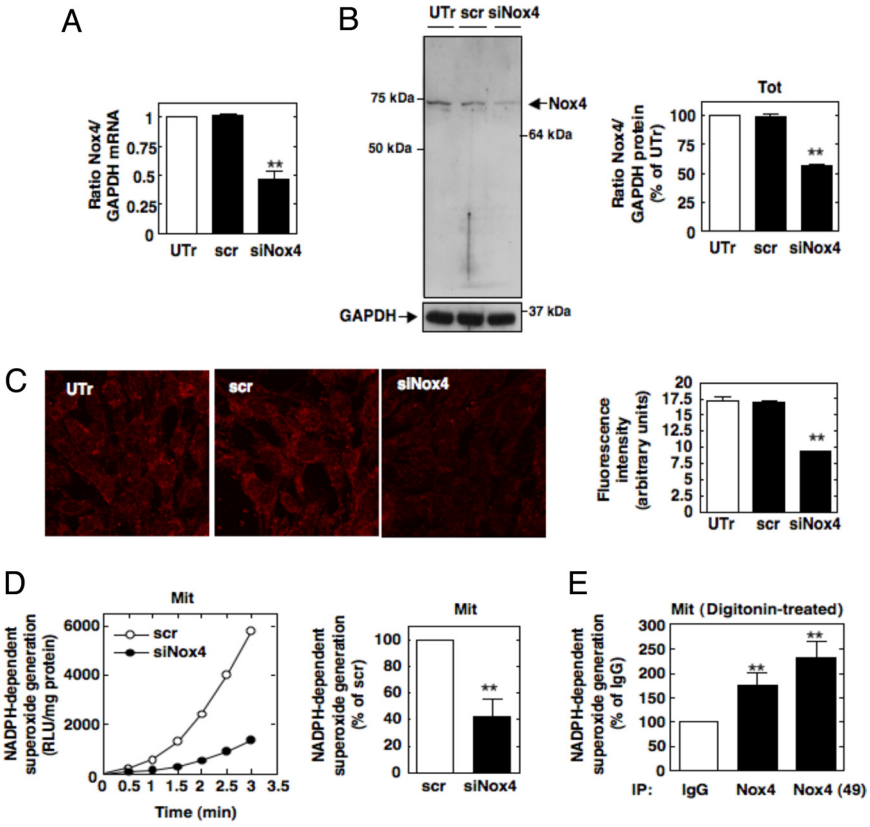

Fig. 4. Mitochondrial Nox4 is functional. (*A*) Nox4 mRNA expression was assessed by real-time PCR in MCs untransfected (UTr) or transfected with Nox4 siRNA (siNox4) or scrambled siRNA (scr). (*B*) Nox4 expression was analyzed by Western blot analysis in total cell lysates from UTr and siNox4- or scr-transfected cells by using our antibody. The histogram represents the ratio of the intensity of Nox4 bands quantified by densitometry factored by the densitometric measurement of GAPDH bands. The data are expressed as percentage of control where the ratio in the control was defined as 100%. Values are the means ± SE from three independent experiments. ##, $P < 0.01$ versus UTr cells. (*C*) Nox4 was visualized by immunofluorescence in UTr and siNox4- or scr-transfected cells with our antibody. Fluorescence intensity was semiquantified, and values are the means ± SE from three independent experiments. **, $P < 0.01$ versus UTr cells. (*D*) NADPH-dependent superoxide generation was measured in pure Mit fraction prepared from siNox4- or scr-transfected cells. Values are the means ± SE from three independent experiments. **, $P < 0.01$ versus scr-transfected cells. (*E*) Digitonin-permeabilized mitochondria were immunoprecipitated by using our Nox4 antibody, the commercial antibody [Nox4 (49)] or IgG control. NADPH-dependent superoxide generation was then measured in the immunoprecipitate. Values are the means ± SE from three independent experiments. **, $P < 0.01$ versus IgG.

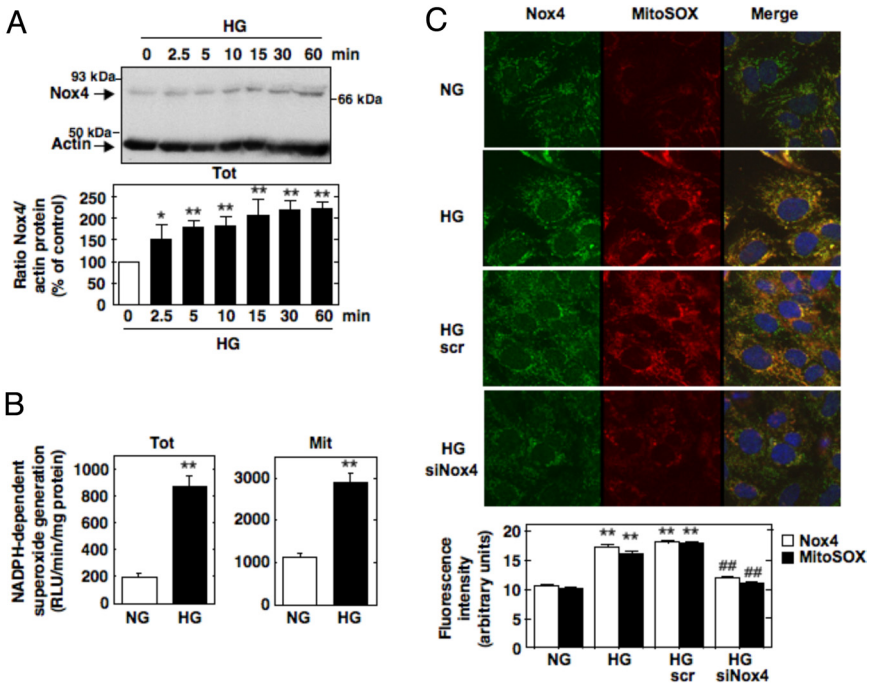

Fig. 5. Mitochondrial Nox4 is involved in glucose-induced ROS generation in MCs. (*A*) MCs were treated with HG for the indicated times. Equivalent amounts of cell lysates were analyzed by Western blot analysis for Nox4 expression by using our antibody. Actin was used as a loading control. The histogram represents the ratio of the intensity of Nox4 bands quantified by densitometry factored by the densitometric measurement of actin band. The data are expressed as percentage of control where the ratio in the control was defined as 100%. Values are the means ± SE from three independent experiments. *, $P < 0.05$ and **, $P < 0.01$ versus control. (*B*) NADPH-dependent ROS generation was measured from total and pure Mit fractions isolated from MCs after exposure to NG or HG for 4 h. (*C*) Representative images obtained by confocal fluorescence microscopy of MitoSOX Red fluorescence in UTr, scr-transfected, and siNox4-transfected MCs after exposure to NG (5 mM D-glucose) or HG (25 mM D-glucose) for 1 h. After fixation and permeabilization, it was cell stained with our Nox4 antibody and appropriate FITC-conjugated secondary antibody. Nuclei were counterstained with DAPI. Fluorescence intensity was semiquantified, and values are the means ± SE from three independent experiments. **, $P < 0.01$ versus NG.

Indeed, the mitochondrial localization probability for Nox4 (97%) was identical to that of the mitochondrial protein human Cyt *c* oxidase subunit IV (COX IV). The cytosolic protein human tuberin was used as a negative control. We next determined whether the mitochondrial Nox4 was functional and active. NADPH-dependent superoxide generation was detected in the Percoll gradient-purified mitochondria from MCs by using lucigenin-enhanced chemiluminescence (Fig. 3). Importantly, NADPH oxidase activity was detected exclusively in fraction 5 of the Percoll gradient (Fig. S3*C*). The activity was inhibited by diphenyleneiodonium (DPI), an inhibitor of Nox oxidases (Fig. 3*A*). It has been recently proposed that Nox4 produces mostly hydrogen peroxide (23, 25, 26). Therefore, we also measured the NADPH-dependent hydrogen peroxide production in Percoll-purified mitochondria by using Amplex red. NADPH-dependent generation of hydrogen peroxide is detected, and is markedly reduced in pure mitochondria prepared from cells pretreated with DPI (Fig. 3*B*).

Transfection of MCs with small interference RNA against Nox4 (siNox4) resulted in down-regulation of Nox4 mRNA as examined by quantitative real-time PCR (Fig. 4*A*), as well as Nox4 protein expression as assessed by immunoblot analysis (Fig. 4*B*). Similarly, the mitochondrial staining pattern of Nox4 is strongly diminished using both our Nox4 antibody and the commercial antibody (Fig. 4*C* and Fig. S5, respectively). NADPH-dependent superoxide generation was significantly reduced in purified mitochondria isolated from siNox4-transfected MCs compared with scrambled siRNA (scr)-transfected cells (Fig. 4*D*). We also show that both independent Nox4 antibodies immunoprecipitate NADPH oxidase activity from digitonin-permeabilized mitochondria (Fig. 4*E*). Together, these data provide evidence that functional Nox4 oxidase is present in mitochondria. Importantly, the observation that NADPH-dependent superoxide generation can be detected in intact mitochondria supports the contention that the carboxyl-terminus of Nox4 NADPH-binding site is most likely positioned in contact with the C or the inner mitochondrial space accessible to the NADPH cofactor. The pores of the outer mitochondria membrane are large enough to allow NADPH to flow within the inner membrane space. However, the inner mitochondrial membrane is impermeable to the flow of NADPH to the inner mitochondrial matrix space. We would like to emphasize that the Percoll-purified mitochondria were intact, supporting these contentions. Intactness of the Mit fraction was demonstrated by showing that NADH oxidase activity was not altered after treatment with rotenone and morphological examination by electron microscopy (Fig. 1*C*; Fig. S6). Interestingly, this concept that Nox4 exists as an active enzyme is in agreement with reports indicating that the Nox4 catalytic subunit generates a significant amount of superoxide in a constitutive manner without the requirement of other membrane or cytosolic subunits essential for the activity of other Nox isoforms such as gp91^{phox}/Nox2 (26, 27).

Oxidative stress is believed to be a major pathogenic mechanism of diabetes complications. The nature of the enzymatic sources of oxidative stress in diabetes or on exposure of cells to high glucose (HG) is not precisely defined. Several studies have reported that overproduction of ROS by the mitochondrial electron-transport chain is responsible for hyperglycemia-induced oxidative stress and the pathogenesis of diabetic complications (2, 4–6). Brownlee (2) and Brownlee and coworkers (5) proposed that this process represents a unified mechanism of diabetic complications. However, recent studies indicate that phagocyte-like NAD(P)H oxidases of the Nox family are also a source of ROS in diabetes (11, 28–30). Glomerular MCs are an important target of HG-induced oxidative damage in diabetes. In MCs, HG elicits ROS generation via the

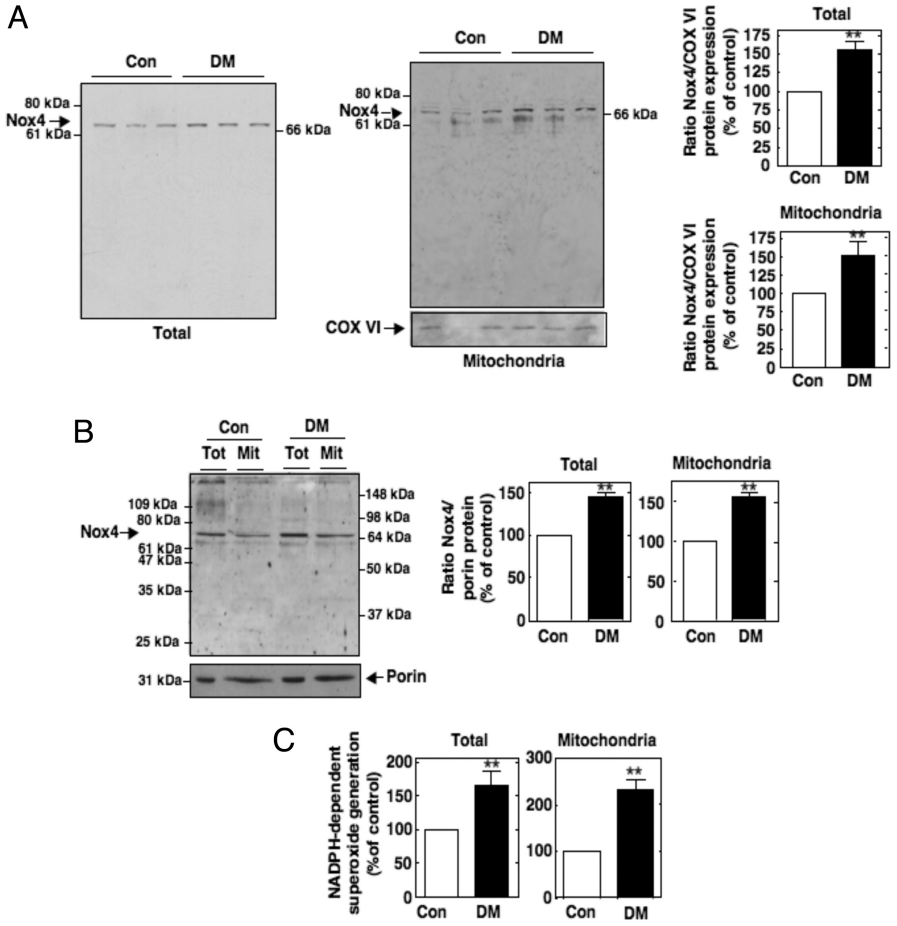

Fig. 6. Regulation of mitochondrial Nox4 in diabetes. (*A*) (*Left*) Immunoblots showing Nox4 protein expression in total cortex homogenate and crude Mit fractions from control (Con) and diabetic (DM) animals. (*Right*) Quantification of Nox4 expression by using our Nox4 antibody in the total and Mit fraction. Cyt *c* oxidase subunit VI (COX VI) was included as a mitochondrial marker. Each histogram represented the ratio of the intensity of Nox4 bands quantified by densitometry factored by the densitometric measurement of COX VI band. Values are the means ± SE from six animals in each group. **, $P < 0.01$ versus control rats. (*B*) Immunoblots showing Nox4 protein expression by using our antibody in total cortex homogenate and Mit fractions from Con and DM animals. Porin was included as a mitochondrial marker. Each histogram represented the ratio of the intensity of Nox4 bands quantified by densitometry factored by the densitometric measurement of porin band. Values are the means ± SE from four animals in each group. **, $P < 0.01$ versus control rats. (*C*) NADPH-dependent superoxide generation was measured in parallel from total and Percoll-purified Mit fractions isolated from the Con or DM rat kidney cortex. Values are the means ± SE from four animals in each group. **, $P < 0.01$ versus control rats.

mitochondrial electron-transport chain (6) and a Nox4-based NAD(P)H oxidase (11). These observations prompted us to investigate the role of mitochondrial Nox4 in these processes. We found that exposure of MCs to HG (25 mM D-glucose) up-regulates Nox4 protein expression (Fig. 5*A*) and increases NADPH-dependent superoxide generation in the total cell homogenate and in the purified Mit fraction (Fig. 5*B*). Studies using MitoSOX Red, a fluorogenic dye detecting selectively mitochondrial superoxide, showed that MitoSOX fluorescence is increased after exposure of MCs to HG (25 mM D-glucose) as compared with cells incubated with normal glucose concentration (NG, 5 mM D-glucose) (Fig. 5*C*). Of interest is that HG-stimulated mitochondrial superoxide generation colocalizes with Nox4. Down-regulation of Nox4 by transfection of the cells with siNox4 prevented the HG-induced increase in mitochondrial superoxide assessed by MitoSOX Red (Fig. 5*C*). Incubation of MCs with the osmotic control, mannitol (20 mM), had no effect on Nox4 protein expression and mitochondrial superoxide generation (Fig. S7). These findings suggest that mitochondrial Nox4 participates in ROS generation induced by HG. We previously reported that renal Nox4 is up-regulated in streptozotocin-induced diabetic rats (11). Here, we show that, in addition to total cortical homogenate, Nox4 protein expression was also increased in crude and Percoll-purified mitochondria isolated from diabetic kidney cortex compared with mitochondria isolated from nondiabetic controls (Fig. 6 *A* and *B*, respectively). The up-regulation of mitochondrial Nox4 protein expression in the diabetic animals was verified by using an independent commercial Nox4 antibody (Fig. S8). Porin was used as a mitochondrial marker. NADPH-dependent superoxide generation was examined in parallel by using the above subcellular fractions from control and diabetic rats. NADPH-dependent superoxide generation was globally increased in the total and pure Mit fractions of the diabetic animals (Fig. 6*C*). This increase in superoxide generation detected in the Mit fraction correlated with the increased mitochondrial Nox4 protein expression. Together, our data suggest that mitochondrial Nox4 contributes to the increase in NADPH oxidase activity in diabetes. Because Nox4 inhibition by antisense oligonucleotides reduced diabetes-induced renal hypertrophy and fibronectin expression (11), the present findings implicate mitochondrial Nox4 in oxidative stress, tissue hypertrophy, and matrix expansion in diabetes.

Our findings may offer an explanation for the evidence in the literature reporting that both mitochondria and Nox-containing oxidases are sources of ROS in pathological states such as

diabetes. Localization of Nox4 to the mitochondria suggests that a short paracrine loop may exist, by which ROS production by mitochondrial Nox4 regulates or is regulated by ROS generation by the mitochondrial respiratory chain. In addition to mitochondrial Nox4, membrane Nox4 is activated by extracellular agonists that bind cell membrane receptors. These observations are consistent with the previous findings that Nox4 contributes to angiotensin II (31) and transforming growth factor-β (32) redox signaling. Our study places Nox4 as a central mediator that controls oxidative stress that may lead to mitochondrial dysfunction and cell injury in diseases such as diabetes. As a corollary to these findings, Nox4 may be considered as a primary target for the design of new therapeutic strategies to counteract oxidant-mediated deleterious effects associated with various diseases characterized by oxidative stress.

Materials and Methods

Materials, cell culture, reagents, previously published methods, RNA interference methods, and immunoprecipitation of NADPH oxidase activity with Nox4 antibodies are described in detail in *SI Methods*.

Animals. Type 1 diabetes was induced in male Sprague–Dawley rats with streptozotocin as described (11), and at day 14 all rats were euthanized.

Subcellular Fractionation. Crude and Mb subcellular fractionation of MCs and kidney cortex was adapted from refs. 12 and 18.

Purification of Mitochondria. Mitochondria were purified from rat kidney cortex or MCs by using a combination of differential and Percoll gradient centrifugation adapted from ref. 19.

ACKNOWLEDGMENTS. We thank D.-Y. Lee and P. Hoover for technical contributions, and J. Barnes for electron microscopy and rabbit immunization. This work was supported by grants from the Juvenile Diabetes Research Foundation Regular research (Y.G. and H.E.A.); a grant-in-aid from the South Central Affiliate of theAmerican Heart Association (Y.G.); the American Diabetes Association (H.E.A.); the National Institutes of Health K01 Award DK 076923 and Grant R01 CA 131272 (K.B.); National Institutes of Health Grants DK 43988 and DK 33665 (H.E.A.); the National Institute of Diabetes and Digestive and Kidney Diseases–National Institutes of Health George O'Brien Kidney Research Center (H.E.A. and Y.G.); and the Veterans Administration (H.E.A. and K.B.).

1. Schnackenberg CG (2002) Oxygen radicals in cardiovascular-renal disease. *Curr Opin Pharmacol* 2:121–125.
2. Brownlee M (2005) The pathobiology of diabetic complications: A unifying mechanism. *Diabetes* 54:1615–1625.
3. Droge W (2002) Free radicals in the physiological control of cell function. *Physiol Rev* 82:47–95.
4. Duchen MR (2004) Roles of mitochondria in health and disease. *Diabetes* 53:S96–S102.
5. Nishikawa T, et al. (2000) Normalizing mitochondrial superoxide production blocks three pathways of hyperglycaemic damage. *Nature* 404:787–790.
6. Kiritoshi S, et al. (2003) Reactive oxygen species from mitochondria induce cyclooxygenase-2 gene expression in human mesangial cells: Potential role in diabetic nephropathy. *Diabetes* 52:2570–2577.
7. Quinn MT, Gauss KA (2004) Structure and regulation of the neutrophil respiratory burst oxidase: Comparison with nonphagocyte oxidases. *J Leukoc Biol* 76:760–781.
8. Geiszt M (2006) NADPH oxidases: New kids on the block. *Cardiovasc Res* 71:289–299.
9. Bedard K, Krause KH (2007) The NOX family of ROS-generating NADPH oxidases: Physiology and pathophysiology. *Physiol Rev* 87:245–313.
10. Geiszt M, Kopp JB, Varnai P, Leto TL (2000) Identification of renox, an NAD(P)H oxidase in kidney. *Proc Natl Acad Sci USA* 97:8010–8014.
11. Gorin Y, et al. (2005) Nox4 NAD(P)H oxidase mediates hypertrophy and fibronectin expression in the diabetic kidney. *J Biol Chem* 280:39616–39626.
12. Nijhawan D, et al. (2003) Elimination of Mcl-1 is required for the initiation of apoptosis following ultraviolet irradiation. *Genes Dev* 17:1475–1486.
13. Kutik S, Guiard B, Meyer HE, Wiedemann N, Pfanner N (2007) Cooperation of translocase complexes in mitochondrial protein import. *J Cell Biol* 179:585–591.
14. Gakh O, Cavadini P, Isaya G (2002) Mitochondrial processing peptidases. *Biochim Biophys Acta* 1592:63–77.
15. D'Alessio M, et al. (2005) Oxidative Bax dimerization promotes its translocation to mitochondria independently of apoptosis. *FASEB J* 19:1504–1506.
16. Soubannier V, McBride HM (2009) Positioning mitochondrial plasticity within cellular signaling cascades. *Biochim Biophys Acta* 1793:154–170.
17. Goyal P, et al. (2005) Identification of novel Nox4 splice variants with impact on ROS levels in A549 cells. *Biochem Biophys Res Commun* 329:32–39.
18. Calamita G, et al. (2005) The inner mitochondrial membrane has aquaporin-8 water channels and is highly permeable to water. *J Biol Chem* 280:17149–17153.
19. Croteau DL, et al. (1997) An oxidative damage-specific endonuclease from rat liver mitochondria. *J Biol Chem* 272:27338–27344.
20. Chen K, Kirber MT, Xiao H, Yang Y, Keaney JF, Jr (2008) Regulation of ROS signal transduction by NADPH oxidase 4 localization. *J Cell Biol* 181:1129–1139.
21. Hilenski LL, et al. (2004) Distinct subcellular localizations of Nox1 and Nox4 in vascular smooth muscle cells. *Arterioscler Thromb Vasc Biol* 24:677–683.
22. Kuroda J, et al. (2005) The superoxide-producing NAD(P)H oxidase Nox4 in the nucleus of human vascular endothelial cells. *Genes Cells* 10:1139–1151.
23. von Löhneysen K, Noack D, Jesaitis AJ, Dinauer MC, Knaus UG (2008) Mutational analysis reveals distinct features of the Nox4–p22 phox complex. *J Biol Chem* 283:35273–35282.
24. Ushio-Fukai M (2006) Localizing NADPH oxidase-derived ROS. *Sci STKE* 2006:re8.
25. Dikalov SI, et al. (2008) Distinct roles of Nox1 and Nox4 in basal and angiotensin II-stimulated superoxide and hydrogen peroxide production. *Free Radic Biol Med* 45:1340–1351.
26. Martyn KD, Frederick LM, von Loehneysen K, Dinauer MC, Knaus UG (2006) Functional analysis of Nox4 reveals unique characteristics compared to other NADPH oxidases. *Cell Signal* 18:69–82.
27. Ambasta RK, et al. (2004) Direct interaction of the novel Nox proteins with p22phox is required for the formation of a functionally active NADPH oxidase. *J Biol Chem* 279:45935–45941.
28. Wendt MC, et al. (2005) Differential effects of diabetes on the expression of the gp91phox homologues nox1 and nox4. *Free Radic Biol Med* 39:381–391.
29. Xia L, et al. (2006) Mesangial cell NADPH oxidase upregulation in high glucose is protein kinase C dependent and required for collagen IV expression. *Am J Physiol* 290:F345–F356.
30. Asaba K, et al. (2005) Effects of NADPH oxidase inhibitor in diabetic nephropathy. *Kidney Int* 67:1890–1898.
31. Gorin Y, et al. (2003) Nox4 mediates angiotensin II-induced activation of Akt/protein kinase B in mesangial cells. *Am J Physiol* 285:F219–F229.
32. Hu T, et al. (2005) ROS production via NADPH oxidase mediates TGF-beta-induced cytoskeletal alterations in endothelial cells. *Am J Physiol* 289:F816–F25.